

Geophysical Research Letters



RESEARCH LETTER

10.1029/2021GL092923

Key Points:

- The previously reported long-term cooling in East Antarctic Plateau from 1 to 1900 CE is only robust between 550 and 1550 CE
- The centennial-scale warm climates occur in 150–250 and 500–800 CE, and cold climates in 1200–1300, 1400–1550, and 1600–1700 CE
- The variability of solar, volcanic, and orbital forcing should be responsible for the long-term cooling and centennial-scale cold climates

Supporting Information:

Supporting Information may be found in the online version of this article.

Correspondence to:

C. An and S. Hou,
anchunlei@pric.org.cn;
shugui@nju.edu.cn






Citation:

An, C., Hou, S., Jiang, S., Li, Y., Ma, T., Curran, M. A. J., et al. (2021). The long-term cooling trend in East Antarctic Plateau over the past 2000 years is only robust between 550 and 1550 CE. *Geophysical Research Letters*, 48, e2021GL092923. <https://doi.org/10.1029/2021GL092923>

Received 10 FEB 2021

Accepted 18 MAR 2021

The Long-Term Cooling Trend in East Antarctic Plateau Over the Past 2000 Years Is Only Robust Between 550 and 1550 CE

Chunlei An^{1,2} , Shugui Hou^{1,3} , Su Jiang² , Yuansheng Li², Tianming Ma⁴, Mark A. J. Curran^{5,6} , Hongxi Pang¹ , Zhaoru Zhang³, Wangbin Zhang¹, Jinhai Yu¹ , Ke Liu¹, Guitao Shi⁷, Hongmei Ma², and Bo Sun²

¹Key Laboratory of Coast and Island Development (Ministry of Education), School of Geography and Ocean Science, Nanjing University, Nanjing, China, ²Key Laboratory for Polar Science (MNR), Polar Research Institute of China, Shanghai, China, ³School of Oceanography, Shanghai Jiao Tong University, Shanghai, China, ⁴School of Earth and Space Sciences, University of Science and Technology of China, Hefei, China, ⁵Division of Australian Antarctic, Channel Highway, Kingston, TAS, Australia, ⁶Australian Antarctic Program Partnership, Institute for Marine and Antarctic Studies, University of Tasmania, Hobart, TAS, Australia, ⁷Key Laboratory of Geographic Information Science (Ministry of Education), School of Geographic Sciences and State Key Laboratory of Estuarine and Coastal Research, East China Normal University, Shanghai, China

Abstract The uncertainties in Antarctic climate reconstructions due to scarcity of proxy records have restricted the understanding of mechanisms of climate change, and further hindered the improvement of climate models. Here, we provide a new climate record derived from water stable isotopes in a Dome A, East Antarctica ice core. Together with six other ice core records, the Dome A record is used to investigate temperature changes in East Antarctic Plateau (EAP) during period 1–1900 CE. Our results show that, a previously reported long-term cooling trend in EAP during the recent (pre-1900 CE) 1900 years is only robust between 550 and 1550 CE. A combination of solar and volcanic forcing may have induced the EAP centennial-scale cold events, and further caused the long-term cooling trend from 550 to 1550 CE with a small contribution from orbital forcing.

Plain Language Summary A surface warming in Antarctica can induce an increase in ice sheet melting and further a rising of global sea level. Therefore, to understand how and why the Antarctic surface temperatures have changed is important to human life. Here, we study the climate variability in East Antarctic Plateau (EAP) during the period of 1–1900 CE. We provide a new climate record from Dome A, the highest ice dome in Antarctica. Using this record and six other climate records from EAP, we find that the previously reported long-term cooling trend in EAP during the recent (pre-1900 CE) 1900 years is only robust between 550 and 1550 CE. We detect warm climate lasting 100 years or more in 150–250 and 500–800 CE, and cold climate in 1200–1300, 1400–1550, and 1600–1700 CE. We suggest that the radiative forcings (solar irradiance, volcanic activity, and orbitally driven insolation) are responsible for the long-term cooling trend from 550 to 1550 CE and the occurrence of centennial-scale cold climate in EAP.

1. Introduction

Temperature-driven changes of the Antarctic ice sheet/shelf might greatly influence the global climate and environment by modulating the sea level and ocean circulation (Alley et al., 2005; Bronselaer et al., 2018; DeConto & Pollard, 2016; Golledge et al., 2019). Therefore, to understand how and why the Antarctic surface temperatures have changed is essential for climate modeling and prediction. The past two millennia, with the availability of high-resolution climate records, provides an appropriate context to investigate both natural and anthropogenic climate forcings (Jones & Mann, 2004; Mann, 2007; Neukom et al., 2019; PAGES 2k Consortium, 2013).

Proxy records are needed to test the validity of climate models due to the short length of Antarctic instrumental temperature records (only since 1950s). The stable isotope composition of water (δD or $\delta^{18}O$) in Antarctic ice cores is a good proxy of past temperature (positive correlation), and it has been widely

© 2021. The Authors.

This is an open access article under the terms of the [Creative Commons Attribution-NonCommercial-NoDerivs](https://creativecommons.org/licenses/by-nc-nd/4.0/) License, which permits use and distribution in any medium, provided the original work is properly cited, the use is non-commercial and no modifications or adaptations are made.

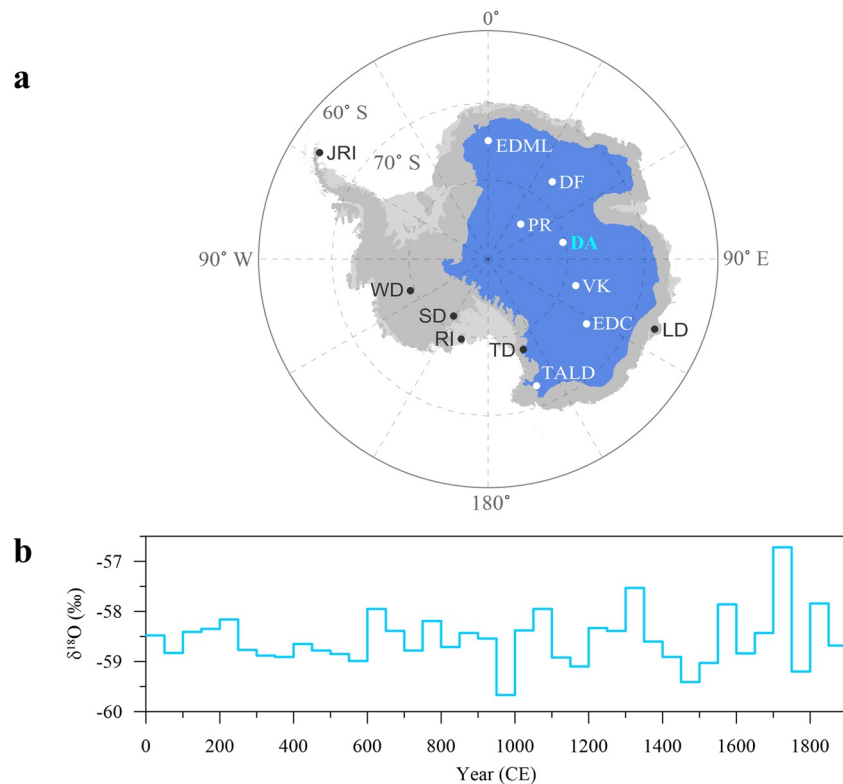


Figure 1. Study area and the new climate record provided by this study. (a) Map of Antarctica showing the locations of ice cores used in this study. The study regions of EAP (with an elevation above 2,000 m) are shown in blue. The white dots indicate records used for the EAP climate reconstruction: DA (Dome A), DF (Dome F), VK (Vostok), PR (Plateau Remote), EDC (EPICA Dome C), EDML (EPICA Dronning Maud Land), and TALD (Tallos Dome). The black dots show other long-term records mentioned in discussion: TD (Taylor Dome), LD (Law Dome), WD (WAIS Divide), SD (Siple Dome), RI (Roosevelt Island), and JRI (James Ross Island). The topographic data were extracted using ETOPO1 global relief data, available from the National Oceanic and Atmospheric Administration at <http://www.ngdc.noaa.gov/mgg/global/global.html>. (b) The profile of DA ice core water stable isotope record ($\delta^{18}\text{O}$) in 50-year resolution.

used to reconstruct the variability of surface temperature in Antarctica over the past two millennia (Goosse et al., 2012; Lüning et al., 2019; PAGES 2k Consortium, 2013; Schneider et al., 2006; Stenni et al., 2017).

The harsh environment of Antarctica limits the availability of ice core records and, consequently, records that cover the past 2000 years are still very sparse. For example, in the latest effort to systematically assess Antarctic temperature variability on regional and continental scales over the past 2000 years (Stenni et al., 2017), a significant cooling trend was found from 1 to 1900 CE in East Antarctic Plateau (EAP), a vast contiguous region with an elevation higher than 2,000 m in East Antarctica (Figure 1a). However, only three EAP records from Dome C, Plateau Remote, and Talos Dome extend into the First Century CE. The relatively small number of records suggests that there might be considerable uncertainties in the climate reconstructions, which could contribute to disagreements between model simulations and proxy reconstructions in Antarctica (PAGES K-PMIP Group, 2015). More records are needed to improve the robustness of these reconstructions.

Here, we present a new $\delta^{18}\text{O}$ record with decadal resolution from a Dome A (DA) ice core. DA is the highest ice dome (80.37°S, 77.37°E, 4,093 m above sea level (a.s.l.)) (Zhang et al., 2007) in Antarctica and near the center of East Antarctica (~1,200 km from the coast, Figure 1a). The thick ice sheet (maximum ice thickness beyond 3,100 m) (Sun et al., 2009) and low snow accumulation rate (21–23 kg m⁻² yr⁻¹) (An et al., 2017) at DA make it easy to get long climate records. The low annual mean temperature (−58°C, firn temperature at 10-m depth) (Bian et al., 2016), low wind speed (2.7 m s⁻¹, 2 m above the ground) (Bian et al., 2016), and extremely slow surface ice flow velocity (11.1 ± 2.4 cm yr⁻¹) (Yang et al., 2014) ensure minimal snow

disturbance after deposition which maximize the preservation of past climate information. Therefore, DA is likely one of the ideal places for paleoclimate reconstruction studies (Hou et al., 2007; Xiao et al., 2008).

To investigate the EAP temperature variability during the period of 1–1900 CE, we combine the DA $\delta^{18}\text{O}$ record with six other $\delta^{18}\text{O}$ records from EAP. Previous studies (PAGES 2k Consortium, 2013; Stenni et al., 2017) have used high resolution (higher than 15 years, and most have annual resolution or higher) records. In this study, records with multi-decadal resolution are included. This study focuses on the long-term climate variability (trends and centennial-scale cold/warm events), and on links between the variability and the factors influencing climates such as solar irradiance, volcanic activity, orbitally driven insolation, and Southern Annular Mode (SAM).

2. Data and Methods

2.1. $\delta^{18}\text{O}$ Records

The DA ice core $\delta^{18}\text{O}$ record has not been previously presented. The 109.91-m ice core was drilled in 2005 and originally dated by various methods (e.g., volcanic time markers, and Herron and Langway firn densification model) (Jiang et al., 2012; Li et al., 2012). Since the results of the previous studies are inconsistent, new dating is needed for this study. Here, the chronology based on volcanic markers from Jiang et al. (2012) is revised using volcanic tie points to a more recently published annual-layer counted volcanic record from the West Antarctic Ice Sheet (WAIS) Divide (WD) ice core (Sigl et al., 2013, 2015, 2016). The maximum age difference between the chronologies of Jiang et al. (2012) and this study is 17 and 9 years for periods 1–1000 and 1000–2000 CE, respectively. Detailed information about the dating can be found in the supporting information (Text S1, Figure S1, Table S1). In this study, we focused on the top 76 m of the core, which covered the past 2000 years. The average sampling resolution is 6 cm (0.9 yr) for the top 1.76 m, and 20 cm (5.3 yr) for the rest of the core. Meltwater $\delta^{18}\text{O}$ was measured with a wavelength scanned cavity ring-down spectroscopy instrument (Picarro L2130i) with an uncertainty of 0.05 ‰.

The other six ice core $\delta^{18}\text{O}$ records used in this paper for the EAP regional climate reconstruction are from Plateau Remote (PR) (Cole-Dai et al., 2000; Mosley-Thompson, 1996; PAGES2k Consortium, 2013), Talos Dome (TALD) (PAGES2k Consortium, 2017; Stenni et al., 2010), EPICA Dome C (EDC) (PAGES2k Consortium, 2017; Stenni et al., 2001), EPICA Dronning Maud Land (EDML), Vostok (VK) and Dome F (DF) (Masson-Delmotte et al., 2011a, 2011b). The locations of the ice cores are shown in Figure 1a. Detailed information of these $\delta^{18}\text{O}$ records is listed in Table S2. All records meet the following requirements: (1) they cover the entire period of 1–1900 CE; (2) the temporal resolution is higher than 25 years. Following Stenni et al. (2017), the record from Taylor Dome (TD), located on the edge of EAP, is also not included in the EAP climate reconstruction, since TD is close to the coast and might be susceptible to coastal impacts.

2.2. Methods

2.2.1. Data Preprocessing

To compare and/or combine the $\delta^{18}\text{O}$ records from different sites, we take an approach to have the records on the same temporal resolution. Each $\delta^{18}\text{O}$ record is resampled in a 50-year resolution by averaging the original data in 50-year bins (as shown in Figure 1b for DA). Then, the resampled data are converted to anomalies relative to the mean over the 1–1900 CE interval (Figure S2). This resampling reduces the data resolution, but weakens the impact of non-climatic noise, for example, effects of post-depositional and wind scouring (Ekaykin et al., 2004; Petit et al., 1982; Stenni et al., 2017; Touzeau et al., 2016).

2.2.2. Compositing Methods

Both unweighted and weighted methods are used to calculate the regional $\delta^{18}\text{O}$ composites. The unweighted composites are produced by calculating the mean $\delta^{18}\text{O}$ anomaly across all records for each 50-yr bin, with no weighting or calibration assumptions. This method applies equal weighting to records from different locations, so it might introduce biases related to the differences between records in their representation of regional climate (Stenni et al., 2017). The weighted method is similar to that introduced by Stenni et al. (2017): a series of weights are applied to ice core $\delta^{18}\text{O}$ anomalies to produce regional anomalies

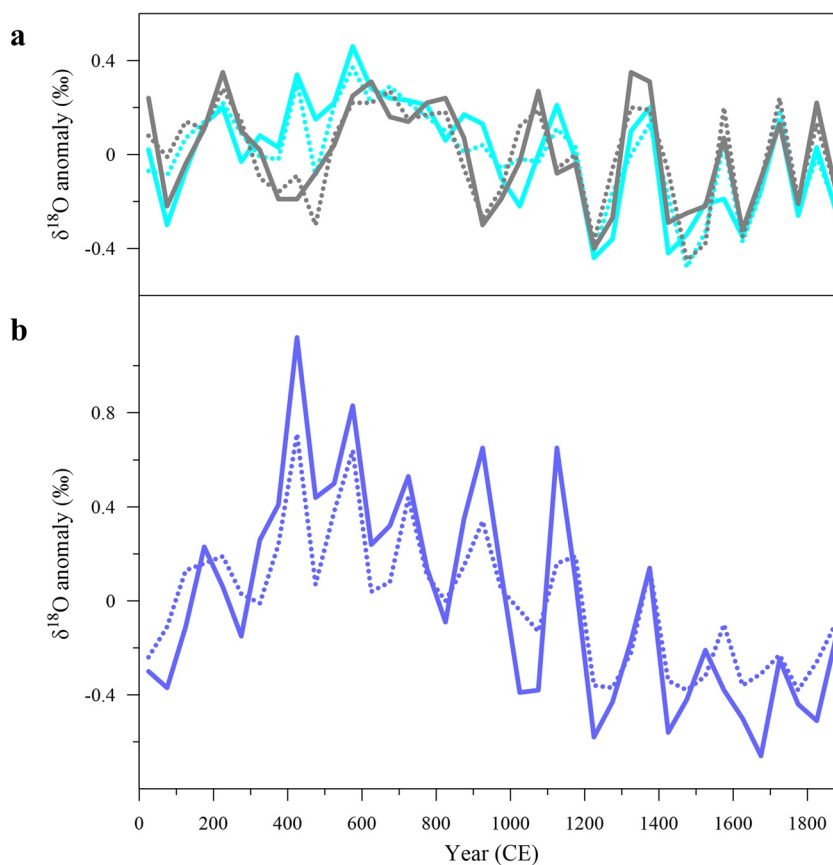


Figure 2. Profiles of composited $\delta^{18}\text{O}$ records (given as anomalies relative to the mean value of 1–1900 CE) of EAP. The solid and dotted lines show the records produced by the weighted and unweighted methods, respectively. (a) Records from this study. The Cyan and gray lines show the CP7 (W and UW, representing the weighted and unweighted composites, respectively) and CP6 (W-PR and UW-PR, representing the weighted and unweighted composites with Plateau Remote record excluded, respectively) records, respectively. Detailed instruction of the names of these records can be found in Sections 2.2.2 and 2.1. (b) The blue lines show the records from Stenni et al. (2017). Here, the original 10-year resolution data are resampled into 50-year resolution.

($\delta^{18}\text{O}_{\text{region}} = \text{weight}_1 * \delta^{18}\text{O}_{\text{site-1}} + \text{weight}_2 * \delta^{18}\text{O}_{\text{site-2}} + \dots + \text{weight}_n * \delta^{18}\text{O}_{\text{site-n}}$). These weights are equal to the corresponding regression coefficients obtained by multiple linear regression between annual mean site temperature and regional (EAP) average temperature over the period of 1958–2012. The surface temperature data set is from Nicolas and Bromwich (2014) (http://polarmet.osu.edu/datasets/Antarctic_recon/).

With the above compositing methods, two composites (named CP7 UW and CP7 W for unweighted and weighted composites, respectively) are produced from the seven $\delta^{18}\text{O}$ anomaly records. To assess the robustness of the regional climate signal presented by these composites, additional $\delta^{18}\text{O}$ composites are produced with the same compositing methods but using six of the seven $\delta^{18}\text{O}$ anomaly records. These 14 composites are referred to as CP6 UW-X or CP6 W-X, in which X represents the record not included in the 6-site composite. The profiles of CP7 and CP6 composites are shown in Figures 2a and S3.

2.2.3. Trend Analysis

The linear regression is the most common method to detect trends in climate variables and has been widely used in past studies (PAGES2k Consortium, 2013; Stenni et al., 2017). It is also applied in this study. The long-term trend in $\delta^{18}\text{O}$ time series is investigated through linear regression analysis, and the trend ($\delta^{18}\text{O}$ -time regression slope) and its statistical significance (p -value, based on the Student's t -test) are calculated.

3. Results and Discussion

3.1. Trends in $\delta^{18}\text{O}$ Time Series

The mean value of the DA $\delta^{18}\text{O}$ records (50-year resolution) in the period of 1–1900 CE is -58.55‰ , which is the lowest in the seven records (Table S3). The standard deviation of the DA $\delta^{18}\text{O}$ record is 0.54‰ , similar to those of DF (0.47‰) and VK (0.51‰) records, larger than those of EDML (0.36‰), EDC (0.34‰), and TALD (0.38‰) records, but much smaller than that of PR (0.88‰) record. No statistically significant ($p < 0.05$) trend over period 1–1900 CE is detected in the $\delta^{18}\text{O}$ records from DA, EDML, VK, and EDC, while a cooling trend is found in records DF, PR, and TALD (Table S4). This result indicates that the climate trend in EAP might be spatially heterogeneous. Interestingly, the above results show a considerable difference between the DA and PR records, both from the EAP sites. The difference may be attributed to the elevation difference at DA (4,093 m a.s.l.) and PR (3,330 m a.s.l.), as well as to the different atmospheric circulation conditions. For instance, Mayewski et al. (2017) suggested that the PR site is located in a region with strong negative meridional wind, while the DA site is located in a transition region between northerly and southerly airflow with much lower annual mean wind speed than the PR site. This difference in atmospheric circulation may lead to considerable difference in air mass and the post-deposition effect between the two sites, and further induce the difference in isotope records.

The composited $\delta^{18}\text{O}$ records are examined to investigate trends of the EAP region. Negative $\delta^{18}\text{O}$ -time slopes, which are statistically significant, are found in the CP7 composites (both UW and W) from 1 to 1900 CE (Table S4). This result seems to imply a regional cooling, which if robust would result in negative $\delta^{18}\text{O}$ -time slopes for all the CP6 composites (Goosse et al., 2012). However, we find that not all the CP6 composites indicate a cooling trend (Table S4). For example, when the PR record is moved, the composites (UW-PR and W-PR) do not show a significant long-term trend (Table S4, Figure 2a).

Stenni et al. (2017) reported a significant long-term cooling in EAP from 1 to 1900 CE. Their reconstructions (Figure 2b) showed significant negative $\delta^{18}\text{O}$ -time slopes, and a Monte Carlo test applied on the unweighted records showed that 99.2% of the 10,000 simulations contained significant cooling trends. Here, we apply the same Monte Carlo test on our unweighted records. In the 10,000 simulated $\delta^{18}\text{O}$ time series (using scaled random Gaussian data which are based on the median value and $\pm 2\sigma$ distribution of data within each 50-year bin of the seven site $\delta^{18}\text{O}$ anomaly records), only 464 (4.6%) simulations show significant cooling trends, and 9,472 (94.7%) simulations do not show a significant long-term trend. The different conclusions from the two studies result from the difference in the selected ice core records. Stenni et al. (2017) used 43 records to produce the composites of EAP. However, in the records they used, only three records cover the past 2000 years: EDC, PR, and TALD, which are also included in our study. We only use long-term records that cover the past 2000 years. The inclusion of DA, VK, and EDML records, all of which show no significant long-term trend, should contribute to the different outcome of regional trends from the two studies.

Next, we investigate long-term trends in 1,000-year time windows. Previous reconstructions (Goosse et al., 2012; PAGES K-PMIP Group, 2015) have found a long-term cooling trend in Antarctica over the last millennium up to 1900, and this cooling trend has also been found in other continents and oceans (McGregor et al., 2015; PAGES 2k Consortium, 2013; PAGES K-PMIP Group, 2015). For comparisons with previous studies of different time coverage (e.g., study period ended in 1800, 1850, or 1900 CE), a trend analysis on $\delta^{18}\text{O}$ composites in a 1,000-year running window is performed in this study. The window starting point steps from 1 to 900 CE, with a step of 50 years. Results (Figure 3) show that none of the composites presents a significant long-term trend in the most recent time windows of 900–1900 CE and 850–1850 CE, and only 2 of the 16 CP6 and CP7 composites (UW-DA and W-DA) show significant regression slopes (negative) in the window of 800–1800 CE.

Our results imply that the EAP seems to be partially isolated from the globally widespread long-term cooling in the past (pre-1900) 1000 or 1900 years. However, detailed inspection of the EAP 1000-year trends shows that, there is only one window (550–1550 CE), in which all CP6 and CP7 composites present significant negative slopes (Figure 3), showing a robust regional cooling trend. To explore factors responsible for these findings, we investigate the centennial-scale climate variability and factors which might influence the EAP climate in the following sections.

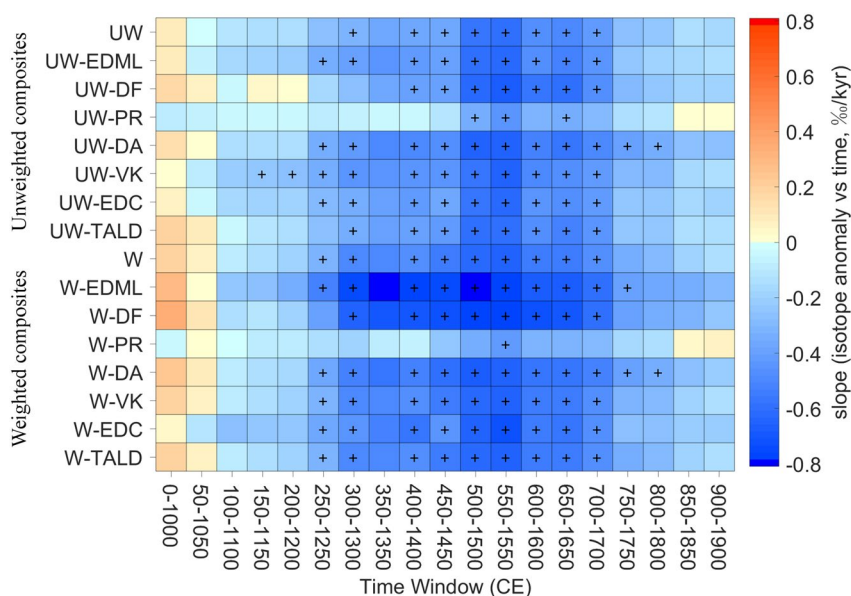


Figure 3. Running trend analysis over a 1,000-year window in period 1–1900 CE for composited $\delta^{18}\text{O}$ records, using 50-year steps. Detailed instruction on the names of these records can be found in Sections 2.2.2 and 2.1. The warm/cold colors show the positive/negative $\delta^{18}\text{O}$ -time slopes, and the black plus signs indicate slopes that are statistically significant.

3.2. Centennial Climate Variability

Some centennial-scale climate episodes in the past 2000 years, for example, Medieval Warm Period and Little Ice Age (LIA), have been widely reported. Medieval Warm Period, also known as the Medieval Climate Anomaly (MCA), is commonly used to indicate the warm climate or climate perturbation during 800–1300 CE (Lamb, 1965; Lüning et al., 2019; Mann et al., 2009). LIA usually refers to the cold climate that occurred between 1300 CE and 1850 CE (Bertler et al., 2011; Grove, 1988; Mann et al., 2009). However, the timing of MCA or LIA is not definitive. Some records suggest that the transition from MCA to LIA could be as early as 1200 CE (Nicolle et al., 2018), and some records show warm climate episodes during LIA (Jones & Mann, 2004; Mann, 2007). The differences in timing and climate patterns of MCA and LIA among regions might indicate that pre-industrial climate forcing was not sufficient to produce globally synchronous extreme temperatures at centennial timescales (Neukom et al., 2019). Here, we investigate the centennial climate events in our reconstructions, and attempt to find links between these events and the long-term trend.

We use the following criteria to detect centennial-scale warm (cold) episodes in EAP during 1–1900 CE: (1) Duration is no less than 100 years; (2) The $\delta^{18}\text{O}$ values in all CP7 and CP6 composites are higher (lower) than the mean value of their series. Using these criteria, we detect two warm episodes (150–250 and 500–800 CE) and three cold episodes (1200–1300, 1400–1550, and 1600–1700 CE), as shown in Figures 4a and 4b. The distribution of these episodes is almost consistent with that on Antarctic continental scales, where the warmest interval occurs between 300 and 1000 CE, and the coldest interval between 1200 and 1900 CE (Stenni et al., 2017). Our results do not show a robust warming during the main period of MCA (1000–1200 CE; Lüning et al., 2019). Though the climate during this period appears relatively warmer than the following cold episodes, the temperature ($\delta^{18}\text{O}$) anomaly is not outstanding in the context of 1–1900 CE. The cold episodes might be an expression of the LIA, indicating a pattern of intermittent cold in EAP during LIA.

Obviously, the transition of high frequency of warm episodes into cold episodes from the first millennium to the second millennium, as indicated by our reconstructions (Figures 4a and 4b), is conducive to the generation of an overall cooling from 1 to 1900 CE. However, the fact that robust cooling is found only in the period of 550–1550 CE suggests that the cold episodes are insufficient to produce a robust cooling trend for the entire 1–1900 CE period.

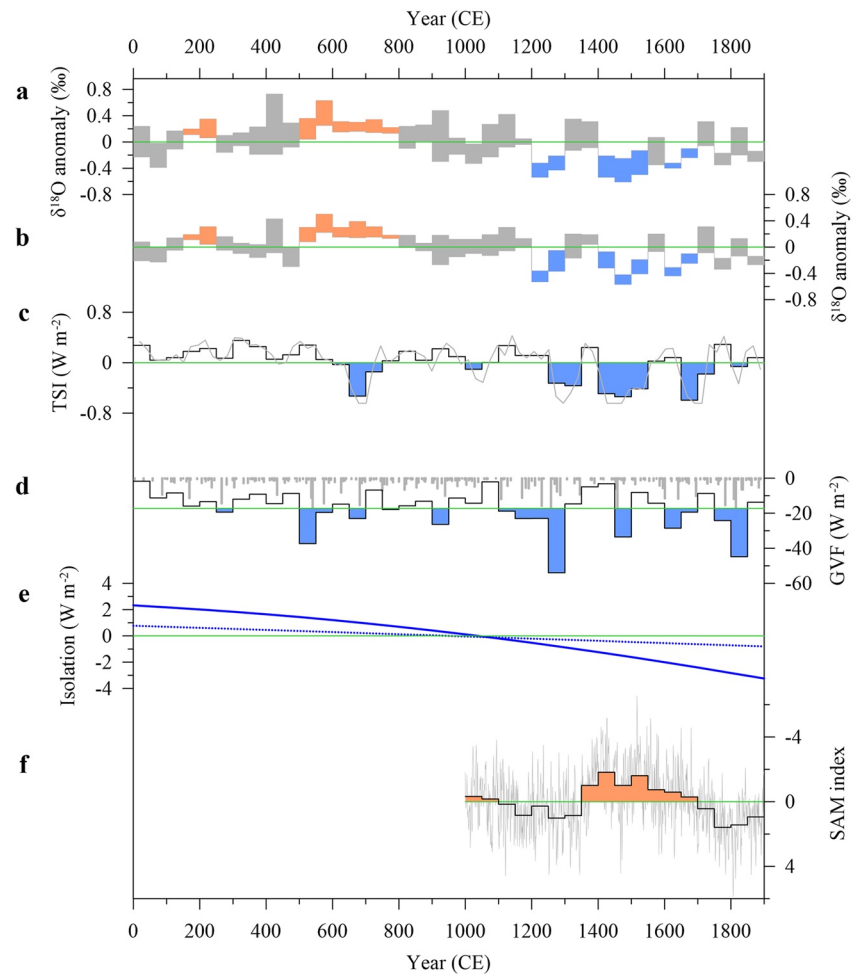


Figure 4. Comparison of EAP regional climate records and factors affecting the climate. The step plots show data in 50-year resolution, and the horizontal green lines indicate the mean value of each series (only for 50-year resolution data in panel d). (a) and (b) Regional $\delta^{18}\text{O}$ reconstructions of EAP by weighted and unweighted methods, respectively, given as the range of $\delta^{18}\text{O}$ anomalies (relative to the mean value of 1–1900 CE) of CP6 and CP7 composites in each 50-year bin, and those indicating robust centennial warm and cold climate state are highlighted in orange and blue, respectively. (c) Total solar irradiance (TSI), the gray line shows the reconstruction of Steinhilber et al. (2012), given as difference to the average value of 1–1900 CE, the black step line shows the average forcing in each 50-year bin, and the blue columns highlight the periods with negative solar forcing. (d) Global volcanic (aerosol) forcing (GVF), the gray bars show the reconstruction of Sigl et al. (2015), the black step line shows the cumulative forcing in each 50-year bin, and the blue columns highlight periods with stronger-than-mean forcings. (e) The orbital-driven change of insolation based on the method of Laskar et al. (2004). The blue solid and dotted line shows the mean insolation of the period with strongest insolation (from November 21 to January 20) and of the whole calendar year. (f) SAM Index. The gray line shows the annual SAM Index reconstructed by Abram et al. (2014), given as difference to the average value of 1–1900 CE, the black step line shows the average Index in each 50-year bin, and the orange columns highlight the periods with negative SAM Index.

3.3. Factors Influencing the EAP Climate in the Past 2000 Years

The main external forcing of climate change in the past 2,000 years are solar irradiance, volcanic activity, orbitally driven insolation, land cover change, and greenhouse gas concentration (Mann, 2007; McGregor et al., 2015; PAGES 2k Consortium, 2013; Schmidt et al., 2011). In addition, the internal variability or dynamics of the climate system, for example, the SAM and El Niño-Southern Oscillation (ENSO), may also influence the regional climate in Southern Hemisphere (Gillett et al., 2006; Lüning et al., 2019). Among the above factors, the impacts of land cover change depend strongly on the location and/or the season, and its effect in Antarctica is suggested to be very small (Bauer et al., 2003; Schmidt et al., 2011, 2012). The

variability of greenhouse gas concentrations was not significant before 1850 (Schmidt et al., 2011, 2012). The influence of ENSO is significant mainly in the Pacific sector of the Antarctic coast and Southern Ocean (Lüning et al., 2019; Turner, 2004). Therefore, we will focus mainly on the influences of the other four factors on the EAP climate.

The decreased solar irradiance has been suggested as one reason for the cold climate in the past 2,000 years (Mann et al., 2009; Orsi et al., 2012). Our results show that, the 1400–1550 EAP cold episode is right in phase with negative solar forcing (Steinhilber et al., 2012) (Figure 4c), indicating a possible close link between this forcing and the EAP climate. However, this forcing alone could not fully explain the occurrence of the other two cold episodes (1200–1300 and 1600–1700 CE).

Compared with the variability of solar forcing, the volcanic forcing is relatively strong (Jones & Mann, 2004). Volcanic activity could induce climate cooling on subdecadal to decadal timescales (Sigl et al., 2015; Stoffer et al., 2015), and even a millennial cooling trend by cumulative effect (increased frequency of volcanic events) (McGregor et al., 2015). The combination of solar and volcanic forcings could explain large part of the pre-industrial (pre-1850) decadal to centennial-scale climate variations (Crowley, 2000; Mann et al., 2009; PAGES 2k Consortium, 2013). Our results indicate that, the volcanic forcing (Sigl et al., 2015) (Figure 4d) could explain the appearance of the 1200–1300 and 1600–1700 but not the 1400–1550 cold stage in EAP, suggesting that only a combination of significant negative solar and volcanic forcing could explain the EAP centennial-scale cold events. Moreover, the warm period of 150–250 CE corresponds to a state of positive solar forcing and weak volcanic forcing. However, the two forcings alone cannot explain the appearance of warm climate in 500–800 CE, during which the two forcings are no higher than their long-term means.

The orbitally driven decrease in local summer insolation has been suggested to be the main driver of the long-term cooling in high northern latitude (Kaufman et al., 2009). However, the insolation change and its effect on climate are strongly dependent on the season and latitude (McGregor et al., 2015). Here, we investigate the isolation change at 80°S (about the middle latitude of EAP) from 1 to 1900 CE. Both the annual mean insolation and the mean value during the period with strongest insolation (from November 21 to January 20) (Laskar et al., 2004) show steady reduction (Figure 4e), indicating that the orbital forcing might be a contributor of the EAP long-term cooling during 550–1550 CE. The reduction in insolation on annual mean is very weak in comparison with the variability of solar and volcanic forcings, suggesting that the effect of orbital forcing might be relatively small on the decadal to centennial timescales during the past two millennia.

The SAM, also known as Antarctic Oscillation, is the major mode of atmospheric circulation variability in the mid and high southern latitudes. There is a close link between the SAM phase and the Antarctic climate over the past 50 years. Negative relationships have been found between the SAM phase and the surface air temperatures of East Antarctica, and positive relationships for the Antarctic Peninsula (Gillett et al., 2006; Kwok & Comiso, 2002; Thompson & Solomon, 2002; Zhang et al., 2018). Though some studies found that the correlation between SAM and the climate of East Antarctica becomes insignificant during 2000–2010 CE (Marshall et al., 2013), the negative relationship is still robust in multi-decadal time windows (e.g., 1958–2012 CE) (Nicolas & Bromwich, 2014). A previous study suggested that the elevated SAM may have intensified the MCA warming observed on the western side of the Antarctic Peninsula (Lüning et al., 2019). If the observed relationship between SAM and EAP climate also applies during the whole period of 1–1900 CE, the weak (negative) SAM phase during 1400–1700 CE, as shown by the reconstruction data (Abram et al., 2014; Dätwyler et al., 2018; Huang et al., 2010, Figure 4f), should result in a relatively warm EAP climate. However, the period of 1400–1700 CE is characterized by cold climate in EAP, in concert with a strong negative radiative forcing (solar and volcanic). In addition, we could not find a clear relationship between SAM and EAP climate for the periods with positive SAM phase. It appears that, on multi-decadal to centennial timescales, the influence of radiative forcings has masked the SAM forced response in EAP before 1900 CE.

The above discussions suggest that the solar and volcanic forcings are the main reason for the EAP centennial-scale cold events and long-term cooling from 550 to 1550 CE. Given the large-scale impacts of these forcings, a widespread long-term cooling in Antarctica during the same period is expected. We also investigate

ice core water isotope records from other Antarctic regions (Figures 1 and S4, Table S2), including Taylor Dome (TD) (Steig et al., 2000; PAGES2k Consortium, 2017), Law Dome (LD) (PAGES 2k Consortium, 2013), WAIS Divide (WD) (Steig et al., 2013; PAGES2k Consortium, 2017), Siple Dome (SD) (Brook et al., 2005; WAIS Divide Project Members, 2013), Roosevelt Island (RI) (Bertler et al., 2017, 2018), and James Ross Island (JRI) (Mulvaney et al., 2012; PAGES2k Consortium, 2017). Indeed, except for two records from low elevation regions in Ross Sea sector (SD, RI), all the other records (WD, TD, LD, JRI) show negative slope (although some are not significant) during 550–1550 CE. On the other hand, this result also supports the previous finding that the ice core water isotope records from low elevation coastal sites could be strongly affected by the nearby oceans (Bertler et al., 2018).

4. Conclusion

Based on seven climate records derived from ice cores in EAP, we have investigated the temperature variability in this region over period 1–1900 CE. A robust long-term cooling appears from 550 to 1550 CE, but this cooling is not robust over the full 1 to 1900 CE period or in any other 1000-year windows in this period. The centennial-scale warm climates happen in 150–250 and 500–800 CE, and cold climates in 1200–1300, 1400–1550, and 1600–1700 CE. The solar and volcanic forcings could explain the majority of the centennial-scale temperature variability of this region, and tend to induce a long-term cooling trend from 550 to 1550 CE. The orbital-driven change of local insolation also makes a small contribution to this cooling trend. Limited by the resolution of our records, this study focused on the long-term climate trend, and centennial variability. In future, high-resolution climate records, which could provide more accurate phase for records comparison and composition, are expected for more detailed studies on climate change and its response to forcings in EAP.

Data Availability Statement

The Dome A isotope data presented here are available from the Global Change Data Repository (<http://www.geodoi.ac.cn/WebEn/doi.aspx?Id=1762>).

Acknowledgments

This study was supported by the Natural Science Foundation of China (41830644, 91837102, 41771031, and 41622605), the Natural Science Foundation of Shanghai (17ZR1433200), the National Key R&D Program of China (2016YFC1400302), the Chinese Arctic and Antarctic Administration (CXPT2020012), and the Chinese National Antarctic Research Expedition. The authors sincerely thank Professor Jihong Cole-Dai for his constructive suggestions. The authors' thanks also go to editor Mathieu Morlighem and two anonymous reviewers for their helpful comments and suggestions.

References

- Abram, N. J., Mulvaney, R., Vimeux, F., Phipps, S. J., Turner, J., & England, M. H. (2014). Evolution of the Southern Annular Mode during the past millennium. *Nature Climate Change*, 4(7), 564–569. <https://doi.org/10.1038/NCLIMATE2235>
- Alley, R. B., Clark, P. U., Huybrechts, P., & Joughin, I. (2005). Ice-sheet and sea-level changes. *Science*, 310(5747), 456. <https://doi.org/10.1126/science.1114613>
- An, C., Wang, Y., & Hou, S. (2017). Glaciological observations at Dome Argus, East Antarctica. *Advances in Polar Science*, 28(4), 245–255. <https://doi.org/10.13679/j.advps.2017.4.00245>
- Bauer, E., Claussen, M., Brovkin, V., & Huenerbein, A. (2003). Assessing climate forcings of the Earth system for the past millennium. *Geophysical Research Letters*, 30(6), 1–9. <https://doi.org/10.1029/2002GL016639>
- Bertler, N. A. N., Conway, H., Dahl-Jensen, D., Emanuelsson, D. B., Winstrup, M., Vallenga, P. T., et al. (2018). The Ross Sea Dipole – Temperature, snow accumulation and sea ice variability in the Ross Sea region, Antarctica, over the past 2700 years. *Climate of the Past*, 14(2), 193–214. <https://doi.org/10.5194/cp-14-193-2018>
- Bertler, N. A. N., Conway, H., Dahl-Jensen, D., Emanuelsson, U., Winstrup, M., Vallenga, P. T., et al. (2017). *Roosevelt Island Climate Evolution (RICE) ice core isotope record*. <https://doi.org/10.1594/PANGAEA.880396>
- Bertler, N. A. N., Mayewski, P. A., & Carter, L. (2011). Cold conditions in Antarctica during the Little Ice Age – Implications for abrupt climate change mechanisms. *Earth and Planetary Science Letters*, 308(1–2), 41–51. <https://doi.org/10.1016/j.epsl.2011.05.021>
- Bian, L., Allison, I., Xiao, C., Ma, Y., Fu, L., & Ding, M. (2016). Climate and meteorological processes of the East Antarctic ice sheet between Zhongshan and Dome-A. *Advances in Polar Science*, 27(2), 90–101. <https://doi.org/10.13679/j.advps.2016.2.00090>
- Bronselaer, B., Winton, M., Griffies, S. M., Hurlin, W. J., Rodgers, K. B., Sergienko, O. V., et al. (2018). Change in future climate due to Antarctic meltwater. *Nature*, 564(7734), 53–58. <https://doi.org/10.1038/s41586-018-0712-z>
- Brook, E. J., White, J. W. C., Schilla, A. S. M., Bender, M. L., Barnett, B., Severinghaus, J. P., et al. (2005). Timing of millennial-scale climate change at Siple Dome, West Antarctica, during the last glacial period. *Quaternary Science Reviews*, 24(12), 1333–1343. <https://doi.org/10.1016/j.quascirev.2005.02.002>
- Cole-Dai, J., Mosley-Thompson, E., Wight, S. P., & Thompson, L. G. (2000). A 4100-year record of explosive volcanism from an East Antarctica ice core. *Journal of Geophysical Research*, 105(D19), 24431–24441. <https://doi.org/10.1029/2000JD900254>
- Crowley, T. J. (2000). Causes of climate change over the past 1000 years. *Science*, 289(5477), 270–277. <https://doi.org/10.1126/science.289.5477.270>
- Dätwyler, C., Neukom, R., Abram, N. J., Gallant, A. J. E., Grosjean, M., Jacques-Coper, M., et al. (2018). Teleconnection stationarity, variability and trends of the Southern Annular Mode (SAM) during the last millennium. *Climate Dynamics*, 51(5), 2321–2339. <https://doi.org/10.1007/s00382-017-4015-0>
- DeConto, R. M., & Pollard, D. (2016). Contribution of Antarctica to past and future sea-level rise. *Nature*, 531, 591. <https://doi.org/10.1038/nature17145>

- Ekaykin, A. A., Lipenkov, V. Y., Kuzmina, I. N., Petit, J. R., MASSON-Delmotte, V., & Johnsen, S. J. (2004). The changes in isotope composition and accumulation of snow at Vostok station, East Antarctica, over the past 200 years. *Annals of Glaciology*, 39(1), 569–575. <https://doi.org/10.3189/172756404781814348>
- Gillett, N. P., Kell, T. D., & Jones, P. D. (2006). Regional climate impacts of the Southern Annular Mode. *Geophysical Research Letters*, 33(23), L23704. <https://doi.org/10.1029/2006GL027721>
- Golledge, N. R., Keller, E. D., Gomez, N., Naughten, K. A., Bernales, J., Trusel, L. D., & Edwards, T. L. (2019). Global environmental consequences of twenty-first-century ice-sheet melt. *Nature*, 566(7742), 65–72. <https://doi.org/10.1038/s41586-019-0889-9>
- Goosse, H., Braida, M., Crosta, X., Mairesse, A., Masson-Delmotte, V., Mathiot, P., et al. (2012). Antarctic temperature changes during the last millennium: Evaluation of simulations and reconstructions. *Quaternary Science Reviews*, 55(6), 75–90. <https://doi.org/10.1016/j.quascirev.2012.09.003>
- Grove, J. M. (1988). *The little ice age*. New York, NY: Methuen.
- Hou, S., Li, Y., Xiao, C., & Ren, J. (2007). Recent accumulation rate at Dome A, Antarctica. *Chinese Science Bulletin*, 52(3), 428–431. <https://doi.org/10.1007/s11434-007-0041-3>
- Huang, J., Wang, S., Gong, D., Zhou, T., Wen, X., Zhang, Z., & Zhu, J. (2010). Atmospheric oscillations over the last millennium. *Chinese Science Bulletin*, 55, 2469–2472. <https://doi.org/10.1007/s11434-010-3210-8>
- Jiang, S., Cole-Dai, J., Li, Y., Ferris, D. G., Ma, H., An, C., et al. (2012). A detailed 2840 year record of explosive volcanism in a shallow ice core from Dome A, East Antarctica. *Journal of Glaciology*, 58(207), 65–75. <https://doi.org/10.3189/2012JG11J138>
- Jones, P. D., & Mann, M. E. (2004). Climate over past millennia. *Reviews of Geophysics*, 42(2), 99–103. <https://doi.org/10.1029/2003RG000143>
- Kaufman, D. S., Schneider, D. P., McKay, N. P., Ammann, C. M., Bradley, R. S., Briffa, K. R., et al. (2009). Recent warming reverses long-term Arctic cooling. *Science*, 325(5945), 1236–1239. <https://doi.org/10.1126/science.1173983>
- Kwok, R., & Comiso, J. C. (2002). Spatial patterns of variability in Antarctic surface temperature: Connections to the Southern Hemisphere Annular Mode and the Southern Oscillation. *Geophysical Research Letters*, 29(14), 50–51. <https://doi.org/10.1029/2002GL015415>
- Lamb, H. H. (1965). The early medieval warm epoch and its sequel. *Palaeogeography, Palaeoclimatology, Palaeoecology*, 1(65), 13–37. [https://doi.org/10.1016/0031-0182\(65\)90004-0](https://doi.org/10.1016/0031-0182(65)90004-0)
- Laskar, J., Robutel, P., Joutel, F., Gastineau, M., Correia, A. C. M., & Levrard, B. (2004). A long-term numerical solution for the insolation quantities of the Earth. *Astronomy & Astrophysics*, 428(1), 261–285. <https://doi.org/10.1051/0004-6361:20041335>
- Li, C., Xiao, C., Hou, S., Ren, J., Ding, M., & Guo, R. (2012). Dating a 109.9 m ice core from Dome A (East Antarctica) with volcanic records and a firm densification model. *Science China Earth Sciences*, 55(8), 1280–1288. <https://doi.org/10.1007/s11430-012-4393-4>
- Lüning, S., Galka, M., & Vahrenholt, F. (2019). The Medieval Climate Anomaly in Antarctica. *Palaeogeography, Palaeoclimatology, Palaeoecology*, 532, 109251. <https://doi.org/https://doi.org/10.1016/j.palaeo.2019.109251>
- Mann, M. E. (2007). Climate over the past two millennia. *Annual Review of Earth and Planetary Sciences*, 35(35), 111–136. <https://doi.org/10.1146/annurev.earth.35.031306.140042>
- Mann, M. E., Zhang, Z., Rutherford, S., Bradley, R. S., Hughes, M. K., Shindell, D., et al. (2009). Global signatures and dynamical origins of the Little Ice Age and Medieval Climate Anomaly. *Science*, 326(5957), 1256–1260. <https://doi.org/10.1126/science.1177303>
- Marshall, G. J., Orr, A., & Turner, J. (2013). A predominant reversal in the relationship between the SAM and East Antarctic temperatures during the twenty-first century. *Journal of Climate*, 26(14), 5196–5204. <https://doi.org/10.1175/JCLI-D-12-00671.1>
- Masson-Delmotte, V., Buiron, D., Ekaykin, A., Frezzotti, M., Gallée, H., Jouzel, J., et al. (2011a). A comparison of the present and last interglacial periods in six Antarctic ice cores. *Climate of the Past*, 7(2), 397–423. <https://doi.org/10.5194/cp-7-397-2011>
- Masson-Delmotte, V., Buiron, D., Ekaykin, A., Frezzotti, M., Gallée, H., Jouzel, J., et al. (2011b). *Water stable oxygen isotope records from six Antarctic ice core sites for the present and last interglacial periods*. PANGAEA. <https://doi.org/10.1594/PANGAEA.785228>. Supplement to: Masson-Delmotte, V et al. (2011): A comparison of the present and last interglacial periods in six Antarctic ice cores. *Climate of the Past*, 7, 397–423. <https://doi.org/10.5194/cp-7-397-2011>
- Mayewski, P. A., Carleton, A. M., Birkel, S. D., Dixon, D., Kurbatov, A. V., Korotkikh, E., et al. (2017). Ice core and climate reanalysis analogs to predict Antarctic and Southern Hemisphere climate changes. *Quaternary Science Reviews*, 155, 50–66. <https://doi.org/10.1016/j.quascirev.2016.11.017>
- McGregor, H. V., Evans, M. N., Goosse, H., Leduc, G., Martrat, B., Addison, J. A., et al. (2015). Robust global ocean cooling trend for the pre-industrial Common Era. *Nature Geoscience*, 8(9), 671–677. <https://doi.org/10.1038/ngeo2510>
- Mosley-Thompson, E. (1996). *Holocene climate changes recorded in an East Antarctica ice core*. Berlin, Heidelberg: Springer.
- Mulvaney, R., Abram, N. J., Hindmarsh, R. C. A., Arrowsmith, C., Fleet, L., Triest, J., et al. (2012). Recent Antarctic Peninsula warming relative to Holocene climate and ice-shelf history. *Nature*, 489, 141–144. <https://doi.org/10.1038/nature11391>
- Neukom, R., Steiger, N., Gómez-Navarro, J. J., Wang, J., & Werner, J. P. (2019). No evidence for globally coherent warm and cold periods over the preindustrial Common Era. *Nature*, 571(7766), 550–554. <https://doi.org/10.1038/s41586-019-1401-2>
- Nicolas, J. P., & Bromwich, D. H. (2014). New reconstruction of Antarctic near-surface temperatures: Multidecadal trends and reliability of global reanalyses. *Journal of Climate*, 27(21), 8070–8093. <https://doi.org/10.1175/JCLI-D-13-00733.1>
- Nicolle, M., Debret, M., Massei, N., Colin, C., Devernal, A., Divine, D., et al. (2018). Climate variability in the subarctic area for the last 2 millennia. *Climate of the Past*, 14, 101–116. <https://doi.org/10.5194/cp-14-101-2018>
- Orsi, A. J., Cornuelle, B. D., & Severinghaus, J. P. (2012). Little Ice Age cold interval in West Antarctica: Evidence from borehole temperature at the West Antarctic Ice Sheet (WAIS) Divide. *Geophysical Research Letters*, 39, L09710. <https://doi.org/10.1029/2012GL051260>
- PAGES 2k Consortium. (2013). Continental-scale temperature variability during the past two millennia. *Nature Geoscience*, 6(5), 339–346. <https://doi.org/10.1038/NNGEO1797>
- PAGES2k Consortium. (2017). A global multiproxy database for temperature reconstructions of the Common Era. *Scientific Data*, 4, 170088. <https://doi.org/10.1038/sdata.2017.88>
- PAGES K-PMIP Group. (2015). Continental-scale temperature variability in PMIP3 simulations and PAGES 2k regional temperature reconstructions over the past millennium. *Climate of the Past*, 11(12), 1673–1699. <https://doi.org/10.5194/cp-11-1673-2015>
- Petit, J. R., Jouzel, J., Pourchet, M., & Merlivat, L. (1982). A detailed study of snow accumulation and stable isotope content in Dome C (Antarctica). *Journal of Geophysical Research*, 87(C6), 4301–4308. <https://doi.org/10.1029/JC087C06p04301>
- Schmidt, G. A., Jungclaus, J. H., Ammann, C. M., Bard, E., Braconnot, P., Crowley, T. J., et al. (2011). Climate forcing reconstructions for use in PMIP simulations of the last millennium (v1.0). *Geoscientific Model Development*, 4(3), 1549–1586. <https://doi.org/10.5194/gmd-4-33-2011>
- Schmidt, G. A., Jungclaus, J. H., Ammann, C. M., Bard, E., Braconnot, P., Crowley, T. J., et al. (2012). Climate forcing reconstructions for use in PMIP simulations of the Last Millennium (v1.1). *Geoscientific Model Development*, 5(1), 185–191. <https://doi.org/10.5194/gmd-5-185-2012>

- Schneider, D. P., Steig, E. J., van Ommen, T. D., Dixon, D. A., Mayewski, P. A., Jones, J. M., & Bitz, C. M. (2006). Antarctic temperatures over the past two centuries from ice cores. *Geophysical Research Letters*, 33(16), 373–386. <https://doi.org/10.1029/2006GL027057>
- Sigl, M., Fudge, T. J., Winstrup, M., Cole-Dai, J., Ferris, D., McConnell, J. R., et al. (2016). The WAIS Divide deep ice core WD2014 chronology – Part 2: Annual-layer counting (0–31 ka BP). *Climate of the Past*, 12(3), 769–786. <https://doi.org/10.5194/cp-12-769-2016>
- Sigl, M., McConnell, J. R., Layman, L., Maselli, O., Mcgwire, K., Pasteris, D., et al. (2013). A new bipolar ice core record of volcanism from WAIS Divide and NEEM and implications for climate forcing of the last 2000 years. *Journal of Geophysical Research: Atmospheres*, 118(3), 1151–1169. <https://doi.org/10.1029/2012jd018603>
- Sigl, M., Winstrup, M., McConnell, J. R., Welten, K. C., Plunkett, G., Ludlow, F., et al. (2015). Timing and climate forcing of volcanic eruptions for the past 2,500 years. *Nature*, 523(7562), 543–549. <https://doi.org/10.1029/2012JD018603>
- Steig, E. J., Ding, Q., White, J. W. C., Küttel, M., Rupper, S. B., Neumann, T. A., et al. (2013). Recent climate and ice-sheet changes in West Antarctica compared with the past 2,000 years. *Nature Geosciences*, 6(5), 372–375. <https://doi.org/10.1038/ngeo1778>
- Steig, E. J., Morse, D. L., Waddington, E. D., Stuiver, M., Grootes, P. M., Mayewski, P. A., et al. (2000). Wisconsinan and Holocene climate history from an Ice Core at Taylor Dome, Western Ross Embayment, Antarctica. *Geografiska Annaler*, 82 A(2–3), 213–235. <https://doi.org/10.1111/j.0435-3676.2000.00122.x>
- Steinhilber, F., Abreu, J. A., Beer, J., Brunner, I., Christl, M., Fischer, H., et al. (2012). 9,400 years of cosmic radiation and solar activity from ice cores and tree rings. *Proceedings of the National Academy of Sciences of the United States of America*, 109(16), 5967–5971. <https://doi.org/10.1073/pnas.1118965109>
- Stenni, B., Buiron, D., Frezzotti, M., Albani, S., Barbante, C., Bard, E., et al. (2010). Expression of the bipolar see-saw in Antarctic climate records during the last deglaciation. *Nature Geosciences*, 4(1), 46–49. <https://doi.org/10.1038/NGEO1026>
- Stenni, B., Curran, M. A. J., Abram, N. J., Orsi, A., Goursaud, S., Masson-Delmotte, V., et al. (2017). Antarctic climate variability on regional and continental scales over the last 2000 years. *Climate of the Past*, 13(11), 1609–1634. <https://doi.org/10.5194/cp-13-1609-2017>
- Stenni, B., Masson-Delmotte, V., Johnsen, S., Jouzel, J., Longinelli, A., Monnin, E., et al. (2001). An oceanic cold reversal during the last deglaciation. *Science*, 293(5537), 2074. <https://doi.org/10.1126/science.1059702>
- Stoffel, M., Khodri, M., Corona, C., Guillet, S., Poulain, V., Bekki, S., et al. (2015). Estimates of volcanic-induced cooling in the Northern Hemisphere over the past 1,500 years. *Nature Geosciences*, 8(10), 784–788. <https://doi.org/10.1038/ngeo2526>
- Sun, B., Siegert, M. J., Mudd, S. M., Sugden, D., Fujita, S., Cui, X., et al. (2009). The Gamburtsev mountains and the origin and early evolution of the Antarctic Ice Sheet. *Nature*, 459(7247), 690–693. <https://doi.org/10.1038/nature08024>
- Thompson, D. W. J., & Solomon, S. (2002). Interpretation of recent Southern Hemisphere climate change. *Science*, 296(5569), 895–899. <https://doi.org/10.1126/science.1069270>
- Touzeau, A., Landais, A., Stenni, B., Uemura, R., Fukui, K., Fujita, S., et al. (2016). Acquisition of isotopic composition for surface snow in East Antarctica and the links to climatic parameters. *The Cryosphere*, 10(2), 837–852. <https://doi.org/10.5194/tc-10-837-2016>
- Turner, J. (2004). The El Niño-southern oscillation and Antarctica. *International Journal of Climatology*, 24(1), 1–31. <https://doi.org/10.1002/joc.965>
- WAIS Divide Project Members. (2013). Onset of deglacial warming in West Antarctica driven by local orbital forcing. *Nature*, 500(7463), 440–444. <https://doi.org/10.1038/nature12376>
- Xiao, C., Li, Y., Allison, I., Hou, S., Dreyfus, G., Barnola, J., et al. (2008). Surface characteristics at Dome A, Antarctica: First measurements and a guide to future ice-coring sites. *Annals of Glaciology*, 48(1), 82–87. <https://doi.org/10.3189/172756408784700653>
- Yang, Y., Sun, B., Wang, Z., Ding, M., Hwang, C., Ai, S., et al. (2014). GPS-derived velocity and strain fields around Dome Argus, Antarctica. *Journal of Glaciology*, 60(222), 735–742. <https://doi.org/10.3189/2014JG14J078>
- Zhang, S., E, D., Wang, Z., Zhou, C., & Shen, Q. (2007). Surface topography around the summit of Dome A, Antarctica, from real-time kinematic GPS. *Journal of Glaciology*, 53(180), 159–160. <https://doi.org/10.3189/172756507781833965>
- Zhang, Z., Uotila, P., Stössel, A., Vihma, T., Liu, H., & Zhong, Y. (2018). Seasonal southern hemisphere multi-variable reflection of the southern annular mode in atmosphere and ocean reanalyses. *Climate Dynamics*, 50(3), 1451–1470. <https://doi.org/10.1007/s00382-017-3698-6>